Tertiary Recycling of Low-Density Polyethylene by Catalytic Cracking over ZSM-11 and BETA Zeolites Modified with Zn²⁺: Stability Study

Laura C. Lerici,*[†,§,∥] María S. Renzini,[†,∥] Ulises Sedran,[‡,§,∥] and Liliana B. Pierella[†,§,∥]

[†]Grupo Zeolitas - CITeQ (Centro de Investigación y Tecnología Química), Facultad Córdoba, Universidad Tecnológica Nacional, Maestro López esquina Cruz roja Argentina S/N (5016) Córdoba, Argentina

[‡]INCAPE (Instituto de Investigaciones en Catálisis y Petroquímica), Facultad de Ingeniería Química, Universidad Nacional del Litoral (FIQ, UNL − CONICET), Santiago del Estero 2654, (S3000AOJ) Santa Fe, Argentina

[§]CONICET (Consejo Nacional de Investigaciones Científicas y Técnicas), Argentina

ABSTRACT: The behavior of Zn-ZSM-11 and Zn-BETA zeolites during the decomposition of low-density polyethylene has been studied in a batch, fixed-bed quartz reactor during successive reaction cycles without catalyst regeneration. The study of the reaction products evolved in the catalytic cracking showed that Zn-ZSM-11 zeolite maintained an essentially stable behavior during all the reaction cycles. On the other hand, Zn-BETA zeolite showed a decrease in the gaseous hydrocarbon fraction. The liquid hydrocarbons disappear after 100 min, and the waxes appear in the last three cycles of polymer cracking, which indicates a behavior similar to thermal degradation. The characterization results (TG, FTIR, and BET surface area) are consistent with the catalytic activity exhibited by both zeolites. The yields of accumulated coke increased steadily throughout the cycles up to maximum values of ∼6.5 and ∼21 wt % for Zn-ZSM-11 and Zn-BETA, respectively. These results were confirmed by TG under air flow.

1. INTRODUCTION

In the last years, the catalytic transformation of waste polymers has appeared as a promising option for converting plastic materials into some valuable chemicals useful as raw materials for the chemical industry or as transportation fuels. These materials are thermally or catalytically degraded into gases and oils. Catalyst addition not only improves the quality of cracking products and lowers the decomposition temperature but also enables a given selectivity to a certain product to be achieved. Because of their physical (textural properties) and their chemical (acid sites) characteristics, zeolites have been extensively used for this reaction. Many examples related to catalytic degradation can be found in the literature.[1−5]

The BETA zeolite (BEA structure) may offer interesting opportunities as a catalyst, since it combines three important characteristics: large pores, high Si/Al synthesis ratio, and a tridirectional network of pores. This zeolite possesses a three-dimensional channel system with 12-membered (12 MR) channel systems. Two topologically identical linear channel systems are mutually orthogonal and perpendicular to the [001] plane; the pore openings of these channels are approximately 6.4 Å × 7.6 Å. A third 12-membered ring channel (5.5 Å × 5.5 Å) is nonlinear and parallel to the c axis; this tortuous channel system is formed by the intersection of the two linear channel systems.

On the other hand, ZSM-11 (MEL structure) zeolites are also interesting to apply this process. The ZSM-11 zeolite structure has two straight channel systems that perpendicularly intersect with apertures formed by a 10-membered ring with a diameter of 5.3 × 5.4 Å. These pores are identical in the directions [100] and [010].

The ion-exchange capacity of zeolite plays an outstanding role. The metal-modified forms of zeolites are important catalysts in many chemical reactions, such as cracking, aromatic alkylation, aromatization, dehydrogenation, and isomerization.[6−9]

Zn species can be introduced into zeolites to increase the rate and selectivity of hydrocarbon conversions, such as aromatization reactions, by inhibiting the undesirable β-scission side reaction.[10−12]

The catalytic properties of the metal are highly dependent upon the interaction between the metal and zeolite and the zeolite structure. Zn²⁺ ions introduced into the zeolites resulted in the partial localization of Zn²⁺ ions at negatively charged tetrahedral AlO₄⁻, which led to a partial decrease in the Brønsted acid sites and obstruction of the remaining bridging OH groups. It is known that there is an increase of the activity for the production of aromatics in the catalytic degradation of polyethylene, in comparison with the metal-free catalyst.[12,13]

The acidic properties of Zn-Beta have been investigated by Kamarudin et al.[14] They found that the presence of Zn²⁺ cations enhanced the catalytic activity of HBEA in n-pentane isomerization due to the presence of strong Lewis acid sites; the sites may facilitate the formation and maintenance of active protonic acid sites through a hydrogen spillover mechanism.

Pierella et al[12] studied the thermal catalytic transformation of HDPE over Zn-, Mo-, and H-, ZSM-11 and MCM-41 materials. These samples could act as an electron-donor−acceptor complex between carbenium intermediate species and the unoccupied molecular orbital (LUMO) of the Zn/Mo sites present in the catalyst by hydride abstraction.

Renzini et al[15] studied the cracking of low-density polyethylene over ZSM-11 modified with H^+ and Zn^{2+}. In this study, they found that Zn^{2+} incorporation favors aromatization due to the higher amount of Lewis acid sites.

A major problem in the use of heterogeneous catalysts is the loss of catalyst activity and/or selectivity in the course of reaction. The changes brought about by catalyst deactivation play a significant, although disadvantageous, role in a large number of important industrial processes.[16] The study of catalyst deactivation is one of the major issues in the practice of catalytic processes. The catalyst cost (type and amount) is an important factor to take into account in the catalyst selection. For this reason, the study of deactivation, regeneration, and reuse of catalysts is of upmost interest from an industrial implementation point of view.[17] Many authors have dealt with this subject in recent years. By contrast, not many studies on Zn-exchanged zeolites have been reported.

Magnoux et al[18] investigated the deactivation by coke of an H-BEA zeolite using the methylcyclohexane model reaction at different temperatures and several contact times. They found that the increasing temperature leads to the formation of highly aromatic coke molecules and to the formation of polyaromatic compounds at 450 °C. Also, the authors showed that bigger crystallite zeolites make coke formation and rapid deactivation easier.

Serrano et al[19] used two samples of H-ZSM-5 zeolite with different textural properties to study the catalyst resistance in the cracking of low-density polyethylene. They found that a reversible deactivation by coke deposition removable by the regeneration procedure and an irreversible or permanent deactivation by other factors occur. However, the improved textural properties of this catalyst is an advantage for the regeneration process, since coke deposited either on the external surface or on the supermicropores and mesopores facilitates the regeneration procedure.

This paper compares the deactivation of Zn-BETA and Zn-ZSM-11 zeolites used in the cracking of low-density polyethylene in a batch fixed-bed reactor, after the repeated use of a given catalyst bed (without regeneration). Zinc cations were introduced into zeolites because of their capability for hydrogen atom transfer, which is a major factor in aromatization that does not affect the unique stability shown by the parent zeolite for this reaction.

2. EXPERIMENTAL SECTION

2.1. Materials. The polymer used in this work was a commercial low-density polyethylene (LDPE) with a melt flow index (determined as the quantity of polymer extruded through a 1 mm die at 190 °C, under a weight of 2.16 kg and for 10 min) of 0.70 g·10 min⁻¹ and a density of 0.922 g·cm⁻³.

The catalysts employed were Zn-ZSM-11 (MEL, Si/Al = 17, named Zn-Z) and Zn-BETA (BEA, Si/Al = 17, named Zn-B) zeolites.

The zeolites were synthesized by means of the hydrothermal crystallization method using tetrabutylammonium hydroxide for the case of the MEL structure[20] and tetraethylammonium hydroxide for the case of the BEA structure[21] as directing agents. The ammonium forms of the zeolite were prepared by ion exchange of the as-prepared Na-zeolite form with 1 M ammonium chloride solution at 80 °C for 40 h. The Zn-zeolites were obtained by the ion exchange of NH_4 samples with 0.5 M zinc nitrate solution by refluxing for 20 h at 80 °C. Finally, the samples were dried at 110 °C and calcined at 500 °C under nitrogen flow and then under an oxidizing atmosphere for 20 h.

2.2. Methods. The catalysts were characterized by different techniques. The Si, Al, and Zn content of the Zn-Z catalyst was determined by atomic absorption spectrometry (AA) in a PerkinElmer AAnalyst 800 spectrometer after microwave digestion of the sample in a Milestone ETHOS 900 digester. In the case of Zn-B, inductive coupled plasma (ICP) in an ICP-OPTIMA 2100 DV PerkinElmer was used.

X-ray powder diffraction (XRD) patterns were collected in air at room temperature on a Phillips PW-1700 equipment, using Cu Kα radiation of wavelength 1.54 Å. Diffraction data were recorded from 5° to 60° 2θ angles, with an interval of 0.01° and a scanning speed of 2°/min.

The assessment of the specific surface areas by the BET method was carried out with N_2 adsorption at 77 K using a Micromeritics ASAP 2000 equipment.

Infrared measurements on the zeolites were performed in a JASCO 5300 FTIR spectrometer. For the structural characterization in the lattice vibration region (400−1800 cm⁻¹), the samples were mixed with KBr at 0.05% and pressed to form wafers.

To determine the type and concentration of acidic sites of the fresh and used (after the successive cycles of reaction) catalysts, pyridine (Py) adsorption experiments were carried out on self-supporting wafers (8−10 mg/cm²) of the Zn-Z and Zn-B zeolites using a thermostatted cell with CaF_2 windows connected to a vacuum line. Pyridine (3 Torr) was adsorbed at room temperature and desorbed at 250, 350, and 400 °C and 10⁻⁴ Torr for 1 h. The number of Brönsted and Lewis acid sites was calculated from the maximum intensity of the adsorption bands at 1545 and 1450−1460 cm⁻¹, respectively, and quantified using the literature data of the integrated molar extinction coefficients, which are independent of the catalysts or strength of the sites.[22] Thermogravimetry experiments in a TGA/SDTA851e/SF/1100 °C Mettler Toledo thermobalance were performed with the polymer alone and its mixtures with both fresh and used catalysts (2/1 mass ratio). To record the maximum rate of mass change as a function of temperature, the experiments were conducted from room temperature to 550 °C at 10 °C/min with a nitrogen flow rate of 30 mL/min. The amount of coke deposited on the catalyst was measured in the above-mentioned thermobalance. These experiments were carried out under air flow of 50 mL/min, and the temperature was changed from 30 to 900 °C with a heating rate of 10 °C/min. The mass loss between 350 and 700 °C was considered to be due to coke burning off.

2.3. Catalytic Activity. The experiments of catalytic degradation were carried out in a batch, fixed-bed quartz reactor (9 mm internal diameter and 300 mm height). The particle size of the catalysts was in the 0.9−1.2 μm range, and the polymer was used as 3.5 mm pellets. The reactor was heated by an electric furnace, which was connected to a programmable temperature controller. A thermocouple was placed very close to the catalyst bed in order to monitor the temperature of the process (Figure 1).

The study of the catalyst stability was performed in different consecutive reaction cycles. In each cycle, the fresh polymer was contacted with the used catalyst from the preceding cycle (i.e., the partially coked catalyst), maintaining the 2/1 polymer-to-catalyst mass ratio, chosen according to previous work.[2] Each experiment started at 25 °C and was heated to 500 °C, holding this final temperature for 20 min. The reaction time of each cycle was 43.75 min. After the reaction time, the reactor was cooled at room temperature before feeding with fresh polymer. The reactor was continuously purged with nitrogen carrier gas at a flow of 25 mL/min.

The gaseous and liquid products were collected and analyzed after each reaction cycle. The liquid yield in each cycle was assessed by weight difference of the condenser before and after the experiment. The mass of coke was determined by weight difference in the reactor, and the mass of gas products was determined by means of an overall mass balance of the experiment. When observed, waxes were quantified together with liquid products.

The reproducibility of the experiments was confirmed by repetition of a number of tests. The polymer was totally converted to gaseous and liquid hydrocarbons (GHC, LHC), waxes, and coke under these conditions, according to the FTIR data of the reactor contents at the end of the experiments, which showed the absence of the band at 1460−1470 cm⁻¹, characteristic of LDPE.
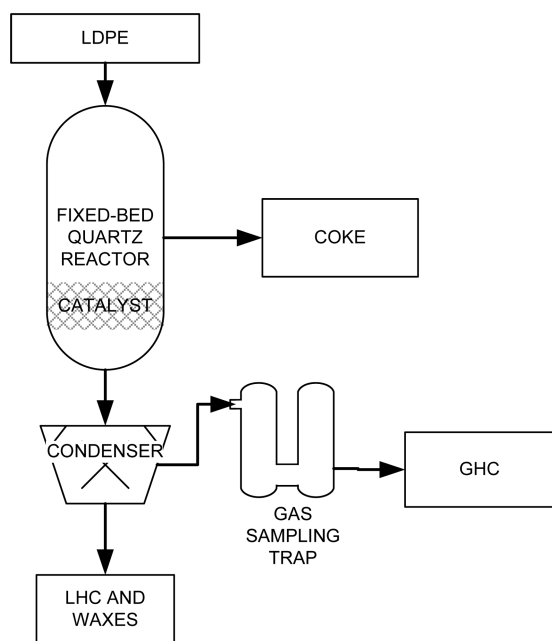
Figure 1. Schematic diagram of the reaction system.

The conversion of the feed is based on the amount of LDPE converted. The reaction temperature and the polymer-to-catalyst mass ratio were specified in order to obtain a 100% polymer conversion in all the cycles with both catalysts. Conversion is defined as the sum of the yields of gaseous hydrocarbons (Y_{GH}), liquid hydrocarbons (Y_{LH}), waxes (Y_W), and coke (Y_C):

$$X \ (\%) = Y_{GH} + Y_{LH} + Y_W + Y_C$$

3. RESULTS AND DISCUSSION

3.1. Characterization of the Fresh and Used Zeolites.
The physicochemical properties of the fresh and used catalysts are summarized in Table 1. It can be seen that the total surface

Table 1. Physicochemical Properties of the Fresh and Used Catalysts

property	fresh catalyst		used catalyst	
	Zn-ZSM-11	Zn-BETA	Zn-ZSM-11	Zn-BETA
Zn (wt %)	2.83[a]	2.90[b]	2.83[a]	2.90[b]
BET surface area (m²/g)	378	585	320	42
crystallinity (%)	>99[c]	>98[c]	>99[c]	>98[c]
	>97[d]	>98[d]	>97[d]	>98[d]
total acid sites (mmol Py/mg)	0.0156	0.0744	0.012	--[e]
Lewis/Brönsted relation	6.45	3.11	7.05	--[e]

[a]AA (atomic absorption). [b]ICP (inductively coupled plasma). [c]XRD (X-ray diffraction). [d]FTIR (fourier transform infrared spectroscopy) in the fingerprint zone of the materials (400–1200 cm⁻¹). [e]--: below the FTIR detection limit.

areas of the fresh Zn-Z and Zn-B catalysts are significantly different, in accordance with observations from other authors.[23] Crystallinity, as assessed by both XRD and FTIR techniques, is very high, thus confirming that the severe conditions employed during the chemical and thermal treatments did not affect the structural characteristics of the catalysts. The XRD patterns of the parent ZSM-11 and BETA catalysts show the characteristic signals corresponding to each structure at 2θ of 7–9° and 23–

24°, and 2θ of 7–8° and 21–22°, respectively (data not shown). No diffraction peaks of ZnO species as an isolated cluster in Zn-zeolites were observed, indicating that the Zn^{2+} cation species in the samples was highly dispersed on the surface of zeolites.

In the case of the used catalyst, coke deposition on the materials decreased the number of total acid sites and changed the Lewis/Brönsted ratio. This effect is more important in Zn-B zeolite, which showed an essentially complete reduction of both the Brönsted and Lewis acid sites.

The surface area of Zn-B zeolite after being run for ∼306 min (seven cycles) decreased sharply from 585 m²/g (fresh catalyst) to 42 m²/g, which corresponds to the disappearance of liquid and the decrease of gaseous yields, and the appearance of waxes shown in Figure 3. On the other hand, Zn-Z zeolite did not show any appreciable change in the surface area value after ∼481 min (11 cycles) of reaction time.

3.2. Catalytic Activity.
Figure 2 shows the weight loss curves obtained in the thermogravimetric analysis (TG curves),
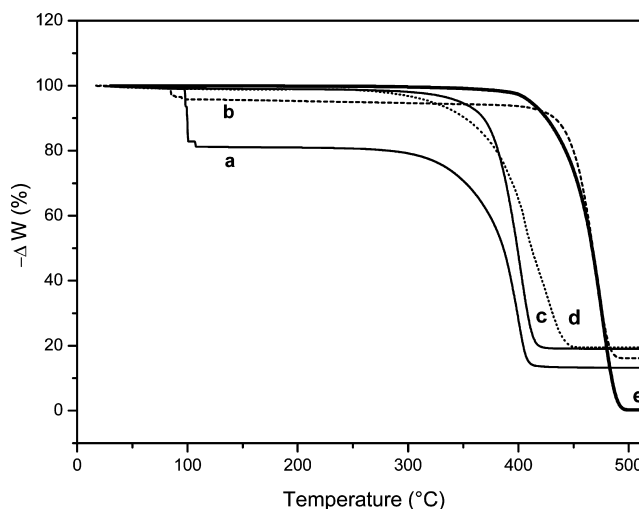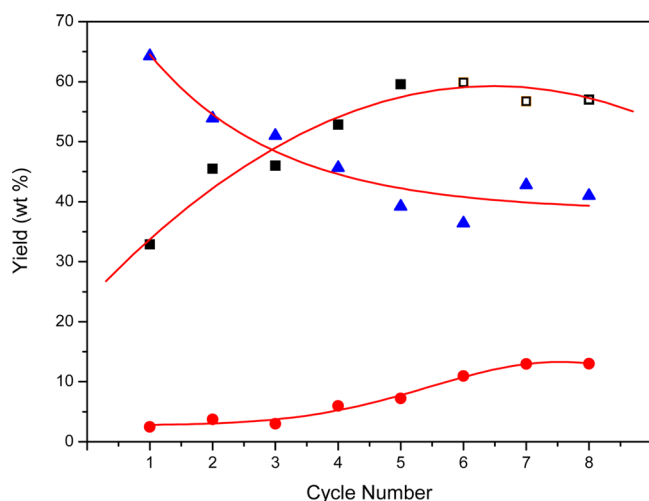

Figure 2. TG profiles of pure LDPE and 2/1 mixtures with fresh Zn-Z and Zn-B zeolites: (a) LDPE/Zn-B fresh; (b) LDPE/Zn-B used; (c) LDPE/Zn-Z fresh; (d) LDPE/Zn-Z used, and (e) LDPE.

corresponding to the degradation of LDPE and its mixtures with fresh and used zeolites. The decomposition temperature of the polymer (without catalyst) is 475 °C. As expected, the presence of fresh zeolites decreases the decomposition temperature in comparison with the purely thermal process. The positive effect of the catalysts is clearly shown by a significant temperature decrease. The Zn-B zeolite shows a higher initial activity, since the difference between the temperatures at the maximum rates of change with and without catalyst, ΔT_{max}, is 76 °C and that for Zn-Z zeolite is 59 °C. A similar behavior was previously observed by using the same matrixes in their protonic form.[24] This behavior is due to a larger surface area and acidity of the BETA zeolite. It has to be considered that the large pores favor the diffusion of the reactants to the active sites. In the case of the used catalyst, TG analyses also reflect a strongly different stability behavior between Zn-Z and Zn-B. It is apparent that the used Zn-Z zeolite exhibited a shift of 59 °C (the same as the fresh catalyst), while the used Zn-B catalyst showed essentially the same degradation temperature profile as the pure polymer.

Figures 3 and 4 show the yield (wt %) of gaseous hydrocarbons (C1−C6), liquid hydrocarbons (C5−C16), waxes (>C20), and coke obtained in the consecutive cycles of LDPE degradation over Zn-B and Zn-Z zeolites without regeneration between tests. The temperature (500 °C) was selected in order to ensure a conversion as high as possible, a fact that, in turn, represents severe conditions to study stability.
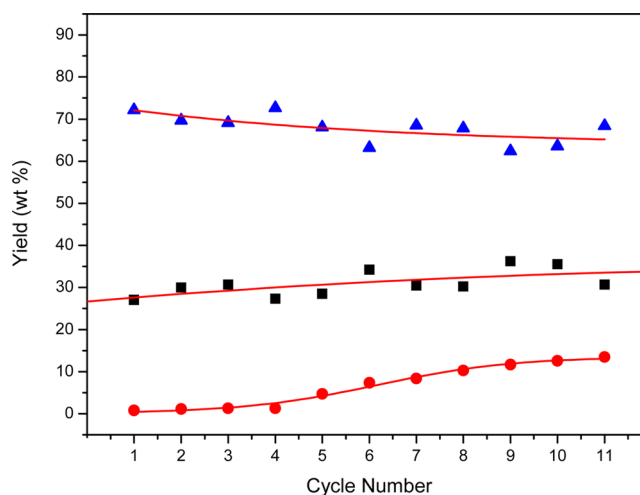
It should be noted that the yield of coke shown for each cycle refers to the total amount of coke accumulated in the catalyst up to this cycle. The thermal cracking of LDPE, performed at 500 °C, only yielded gas (∼38 wt %), wax (∼61 w%), and coke (0.74 wt %) products. It should be noted that there were no liquid products during this test. In the case of Zn-B zeolite, it can be seen (Figure 3) that the yield of GHC decreased from

Figure 4. Yields of the products obtained in the consecutive cycles of LDPE conversion over Zn-Z zeolite. Symbols: (red circle) accumulated coke; (black square) liquid products; (blue triangle) gaseous products.

The thermogravimetric analyses of the catalysts used after consecutive reactions were carried out to estimate the amount of coke deposited on the zeolites. The corresponding differential thermograms are shown in Figure 5 and reveal

Figure 3. Yields of the products obtained in the consecutive cycles of LDPE conversion over Zn-B zeolite. Symbols: (red circle) accumulated coke; (black square) liquid products; (blue triangle) gaseous products; (white square) waxes.
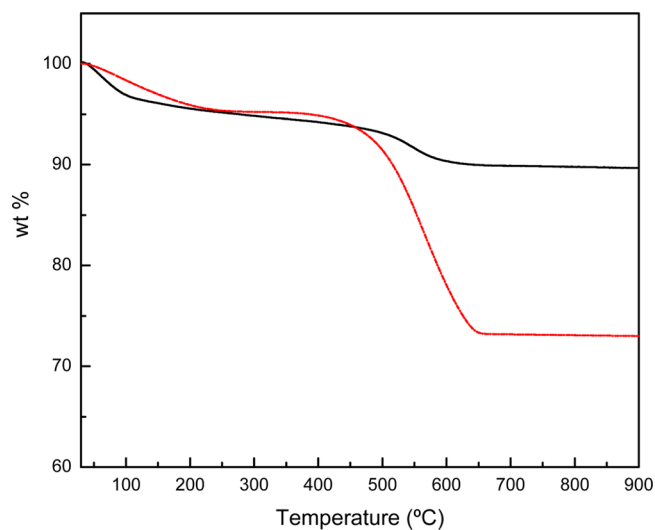
approximately 64 wt % to about 41 wt % in the eighth cycle; on the contrary, the yield of LHC exhibited a tendency to increase from 33 to 59 wt % in the fifth cycle. It should be noted that there were no liquid products from the sixth cycle. The average wax yield was about 57 wt % in the last three cycles. Because of the similarity with the thermal cracking behavior observed in the last three cycles, the study was finished in the seventh cycle. These results show that the catalyst has lost its activity, yielding waxes and gases almost in the same proportion as in the thermal run. This deactivation has also been observed by other authors, and it has been associated with coke deposition, which seems to block the zeolite pores as well as the acid sites.[25] However, cracking products were observed in the last cycles, which would be due to a temperature effect. This is evident in the FTIR and TG analyses made to the catalyst used (Figures 2 and 6). The accumulation of coke deposits on the surface could also be the reason for the deactivation of Zn-B.

Figure 4 shows that the Zn-Z zeolite maintained an essentially stable behavior during all the reaction cycles, with average yields of 28 wt % of LHC and 67 wt % of GHC. Moreover, it was observed that the Zn-Z zeolite did not form waxes among the products. The results essentially indicate no deactivation of the catalyst. Zn-Z has thus been shown to have a stable yield profile in the degradation of polyethylene, which is beneficial in terms of its practical use.

Figure 5. Coke TG profiles of used Zn-Z (black line) and Zn-B (red dashed line).

coke contents of 6.5% and 21.83% for Zn-Z and Zn-B, respectively. Peaks at about 542 and 561 °C were found in Zn-Z and Zn-B, respectively. These disparities observed in the combustion behavior of the coked catalysts suggest structural differences in the nature of the coke obtained in both samples.[26]

The differences in the behaviors of the two zeolites in the conversion of LDPE can be associated with the stability properties of each material in handling these catalytic cracking reactions. In effect, experimental evidence shows the influence of shape selectivity on the deactivation of zeolites by coke, Zn-Z zeolite showing lower coke yields. Since bimolecular reactions (condensation, hydrogen transfer) between bulky molecules are

involved, steric constraints limit the formation of highly condensed molecules in the zeolite pores.

The catalytic cracking of polyolefins can be described as made up of the following steps. The plastic first melts, and then the polymeric chains react to form waxes through a radical mechanism. This mechanism is nonspecific and occurs all over the reactor bed similarly to a reaction without catalyst, which only yields waxes.[27,28] The wax molecules, subjected to diffusional restrictions, can reach the catalyst acid sites in the zeolite, where they react through well-known carbocation chemistry, and due to their paraffinic nature, the most probable intermediate in the conversion of waxes is a protonated cyclopropane entity.[29]

The coke deposited on Zn-Z can be considered as the association of a small number of aromatic rings with numerous and long aliphatic chains attached. However, Zn-B possesses a three-dimensional pore system with straight channels of 0.73 nm × 0.65 nm and tortuous channels of 0.55 nm × 0.55 nm with 1.0 nm channel intersections. These channel intersections probably allowed the trapping of coke precursor and resulted in the formation of bulky carbonaceous compounds with the polyaromatic character. Therefore, it can be deduced that the Zn-Z zeolite pore system limits more severely the condensation reactions, resulting in a less pronounced formation of coke and, consequently, a lower deactivation than that of Zn-B zeolite.

The results show that acid zeolites generate carbon deposition on the acid sites. In the particular case of BEA zeolite, a greater amount of coke is produced due to the 12-ringed pore system. The low coking properties of ZSM-11 zeolite are due to its specific structure and relatively small pore size that do not allow deposition of large cracked molecules into the pores compared to the other zeolite types.[4,30] These observations could be explained by assuming the occurrence of pore blocking by coke deposited in the one-dimensional channels of zeolite. Zn-B has very strong acid sites (determined by pyridine FTIR desorbed at 400 °C) and large pores that favor the formation of coke. The amount of coke produced blocks the entrance of the one-dimensional pores, resulting in a decrease in the accessibility to the acid sites remaining intact in the channels, that is, a lowering of the catalytic activity.

The FTIR spectra of pyridine adsorbed on fresh and used Zn-Z and Zn-B catalysts are shown in Figure 6 (1400–1700 cm^{-1} zone).

A band can be seen at 1638 cm^{-1}, which is assigned to structural OH$^-$ ion vibration,[31] indicative of the interaction of pyridine with Brönsted acid sites (PyH$^+$). The Zn-zeolites present an intense signal at 1614 cm^{-1} that could be related to new Lewis acid sites (electron donor–acceptor, EDA) generated by zinc incorporation.[20,32] The position of the bands close to 1600 cm^{-1} can be considered as an indication of the Lewis acid strength of the surface sites.[33] Bands at higher wavenumbers (1620–1623 cm^{-1}) would result from strong Lewis sites, whereas bands at lower wavenumbers (1614 cm^{-1}) would indicate medium to strong sites.

Bands at 1455, 1490, and 1545 cm^{-1} can be observed in both fresh samples. The band at 1490 cm^{-1} corresponds to the vibration of pyridine adsorbed over Brönsted and Lewis acid sites. The band at 1455 cm^{-1} corresponds to the interaction of pyridine with Lewis acid sites (PyL), and the band at 1545 cm^{-1} is indicative of the interaction of pyridine with Brönsted acid sites (PyH$^+$).[31,34]

The results of the pyridine FTIR analysis of the fresh and used zeolites can be associated with the performance of each
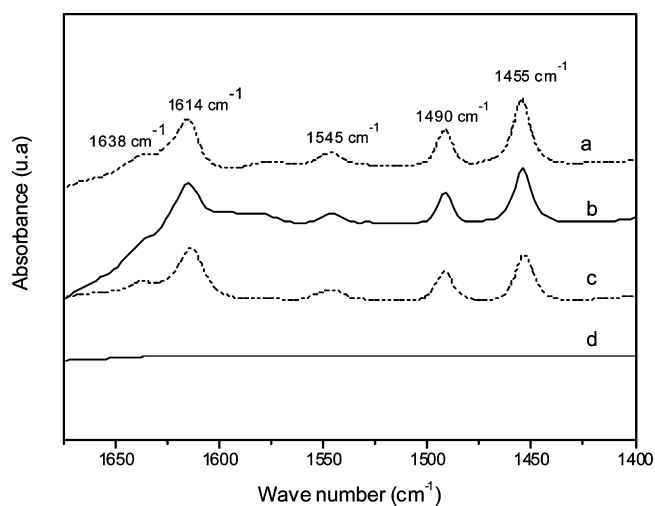

Figure 6. FTIR spectra of pyridine adsorbed on the catalysts: (a) fresh Zn-Z; (b) used Zn-Z; (c) fresh Zn-B; (d) used Zn-B.

catalyst in the experiments of catalytic activity (Figure 6). In effect, the Zn-Z zeolite exhibited stable yields during the successive cycles of LDPE conversion, which could be supported by the not so important decline in the number of acid sites observed in this catalyst. On the contrary, the Zn-B zeolite showed a significant decrease in yields and an almost complete loss of total acid sites at the seventh cycle.

The previous results (TG, FTIR, and BET surface area) are consistent with the catalytic activity exhibited by both zeolites (Figures 3 and 4). Coke formation affects catalyst activity and also product distribution (Figures 7, 8, and 9). This effect could be due to the poisoning or consuming active sites and/or the blocking of catalyst pore channels.[35]

Another interesting point to note is product distribution. In Figure 7, it is shown that Zn-Z produced a higher proportion of C3−C4 hydrocarbons, whereas Zn-B produced a higher percentage of the C5−C6 fraction. This different behavior can be explained taking into account that the pore size of Zn-B zeolite is larger than that of Zn-Z zeolite. Accordingly, the Zn-B zeolite shows higher selectivity to products with a higher
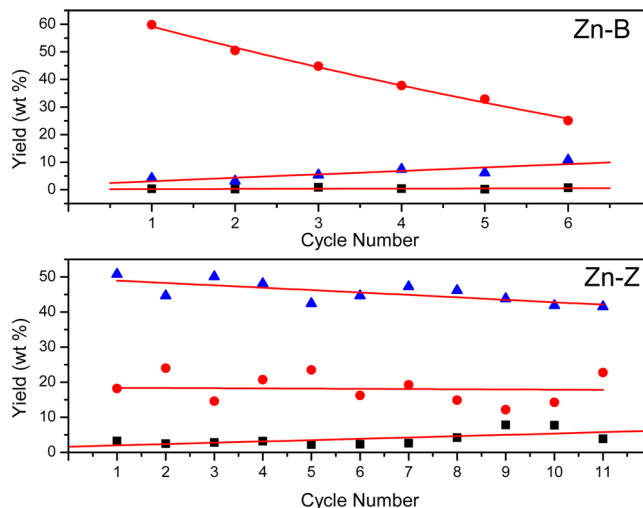
Figure 7. Gaseous product distribution of the LDPE catalytic degradation over Zn-B and Zn-Z. Symbols: (black square) C1−C2; (blue triangle) C3−C4; (red circle) C5−C6.
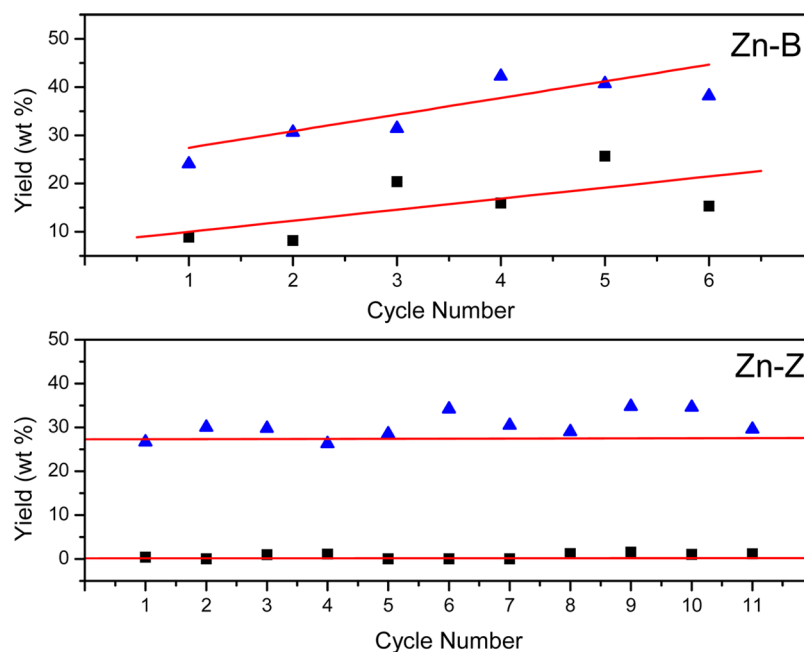
Figure 8. Distribution of gasoline (blue triangle) and diesel (black square) in the liquid fraction obtained over Zn-B and Zn-Z zeolites.

number of carbon atoms. Similar results have been reported by other authors.[4,36]

The evolution of the yield of gaseous products during the different cracking runs is another important fact to analyze. It can be noticed that Zn-Z maintained a stable production during all the cycles, whereas Zn-B presented an important decrease of the C5−C6 fraction produced by the effect of increased coke deposited over the zeolite surface.

Figure 8 gives the yields of gasoline (C5−C10) and diesel (C11−C16) obtained for both Zn-B and Zn-Z zeolites. It can be seen that the yields of gasoline obtained for Zn-Z showed a slight increase (from 26 to 33 wt %), whereas the diesel fraction remained practically constant during the 11 cycles of reaction. On the other hand, Zn-B produced higher diesel percentages that increased with the progressive cycles from about 9 to 15 wt % in the last run. The yield of gasoline showed a slight increase from ∼24 to 38 wt %. The high yield of gasoline produced for both zeolites is worth noticing.

The aromatic (C6−C9) and coke yields generated in each cycle of LDPE cracking over Zn-B and Zn-Z zeolites are shown in Figure 9. This is another interesting point to discuss because the aromatic components produced an increase in the octane index.[37] However, the yields of aromatics in gasoline must be limited to reduce toxic air emissions. In this sense, both zeolites generate interesting cuts to formulate gasoline in the refineries.

On the other hand, the increase in the Lewis active sites generated by the incorporation of Zn promoted the significantly high production of C6−C9 aromatic hydrocarbons in both zeolites. These facts may be explained by the known selective formation of aromatics over Lewis acid sites by a combination of cyclization and hydrogen transfer processes.[38]

It can be seen in Figure 9 that the amount of coke generated in each cycle is approximately the same. It should be noted that the yield of coke shown for each cycle refers to the individual amount of coke generated in each cycle and not the accumulated presented in Figures 3 and 4. This behavior can be observed in both catalysts. Although the yield of C6−C9 aromatics is also approximately constant in each cycle (which is
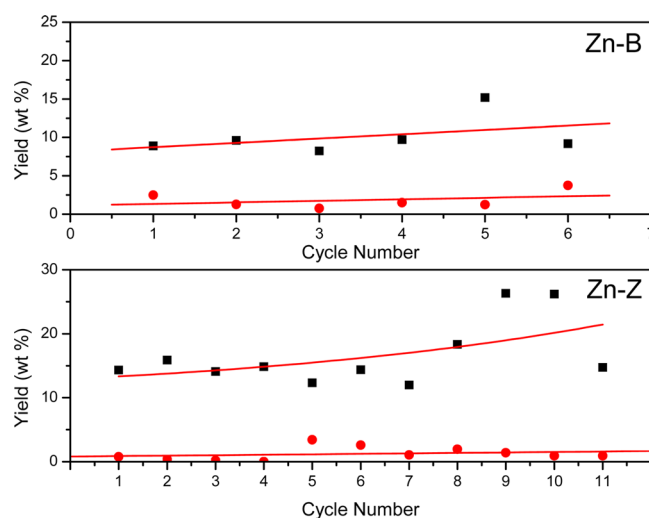
Figure 9. Aromatic and individual coke yields obtained over Zn-B and Zn-Z zeolites. Symbols: (black square) aromatic; (red circle) individual coke.

particularly noticeable in catalyst Zn-B), we think that it is not possible to expect a clear correlation between the yields of these products and coke formation. Indeed, coke in this process is the result of very complex processes inside the zeolite pore structure, where aromatics may play an important role; however, many other hydrocarbon product (i.e., olefins) are also contributors.[4]

The highest content of aromatic hydrocarbons observed in Zn-Z is due to a distinctive combination of pore systems and acidity (high relation L/B).

4. CONCLUSIONS

The results obtained in the present work reflect the performance of Zn-BETA (Zn-B) and Zn-ZSM-11 (Zn-Z) zeolites during LDPE cracking, showing a good correspondence

between the catalytic activities of the solids and their acidic and structural properties.

The Zn-Z zeolite maintained a stable behavior during the 11 reaction cycles, with average yields of 28 wt % of LHC and 67 wt % of GHC, and without noticeable changes in the product distribution.

The performance of Zn-B zeolite was completely different. The yield of GHC decreased from approximately 64 wt % to about 41 wt % in the eighth cycle; on the contrary, the yield of LHC exhibited a tendency to increase from 33 to 59 wt % in the fifth cycle. It should be noted that there were no liquid products from the sixth cycle. The average wax yield was about 57 wt % in the last three cycles, similar to thermal cracking.

The deposition of coke on Zn-B zeolite caused an essentially complete loss of both Brönsted and Lewis acid sites. The shape selectivity of Zn-Z zeolite mitigates the deactivation by coke deposition in the catalytic transformation of polymers.

■ AUTHOR INFORMATION

Corresponding Author

*Tel: +54 0351 4690585. Fax: +54 0351 4690585. Email: llerici@scdt.frc.utn.edu.ar, laulerici@hotmail.com.

Author Contributions

‖These authors contributed equally. The manuscript was written through contributions of all authors. All authors have given approval to the final version of the manuscript.

Notes

The authors declare no competing financial interest.

■ ACKNOWLEDGMENTS

■ REFERENCES

(1) Aguado, J.; Serrano, D. P.; Escola, J. M.; Garagorri, E.; Fernández, J. A. *Polym. Degrad. Stab.* **2000**, *69*, 11−16.

(2) Renzini, M.; Sedrán, U.; Pierella, L. *J. Anal. Appl. Pyrolysis* **2009**, *86*, 215−220.

(3) Lin, H.; Yang, M.-H. *J. Anal. Appl. Pyrolysis* **2008**, *83*, 101−109.

(4) Manos, G.; Garfoth, A.; Dwyer, J. *Ind. Eng. Chem. Res.* **2000**, *39*, 1198−1202.

(5) Durmuş, A.; Naci Koc, S.; Selda Pozan, G.; Kaşgöz, A. *Appl. Catal., B* **2005**, *61*, 316−322.

(6) Konno, H.; Okamura, T.; Kawahara, T.; Nakasaka, Y.; Tago, T.; Masuda, T. *Chem. Eng. J.* **2012**, *207−208*, 490−496.

(7) Smiesková, A.; Hudec, P.; Kumar, N.; Salmi, T.; Yu Murzin, D.; Jorík, V. *Appl. Catal., A* **2010**, *377*, 83−91.

(8) Gounder, R.; Iglesia, E. *J. Catal.* **2011**, *277*, 36−45.

(9) Lima, P. M.; Garetto, T.; Cavalcante, C. L.; Cardoso, D., Jr. *Catal. Today* **2011**, *172*, 195−202.

(10) Biscardi, J. A.; Meitzner, G. D.; Iglesias, E. *J. Catal.* **1998**, *179*, 192−202.

(11) Anunziata, O. A.; Pierella, L. B. *Catal. Lett.* **1992**, *16*, 437−441.

(12) Pierella, L. B.; Renzini, M. S.; Anunziata, O. A. *Microporous Mesoporous Mater.* **2005**, *81*, 155−157.

(13) Aguado, J.; Serrano, D. P.; Escola, J. M. *Ind. Eng. Chem. Res.* **2008**, *47*, 7982−7992.

(14) Kamarudin, N. H. N.; Jalil, A. A.; Triwahyono, S.; Mukti, R. R.; Ab Aziz, M. A.; Setiabudi, H. D.; Mohd Muhid, M. N.; Hamdan, H. *Appl. Catal., A* **2012**, *431− 432*, 104−112.

(15) Renzini, M. S.; Sedrán, U.; Pierella, L. B. *J. Anal. Appl. Pyrolysis* **2009**, *86*, 215−220.

(16) Kumbilieva, K.; Petrov, L.; Alahamed, Y.; Alazahrani, A. *Chin. J. Catal.* **2011**, *32*, 387−404.

(17) Forni, L.; Solinas, V.; Monaci, R. *Ind. Eng. Chem. Res.* **1987**, *26*, 1860−1864.

(18) Magnoux, P.; Rabeharitsara, A.; Cerqueira, H. S. *Appl. Catal., A* **2006**, *304*, 142−151.

(19) Serrano, D. P.; Aguado, J.; Rodríguez, J. M.; Peral, A. *J. Anal. Appl. Pyrolysis* **2007**, *79*, 456−464.

(20) Anunziata, O.; Pierella, L. *Catal. Lett.* **1993**, *19*, 143−151.

(21) Valencia, S.; Camblor Fernandez, M. A.; Corma, A.; Perez, J. U.S. Patent 2,124,142.

(22) Emeis, C. A. *J. Catal.* **1993**, *141*, 347−354.

(23) Aguado, J.; Serrano, D.; Escola, J.; Garagorri, E.; Fernández, J. *Polym. Degrad. Stab.* **2000**, *69*, 11−16.

(24) Renzini, M. S.; Lerici, L. C.; Sedrán, U.; Pierella, L. B. *J. Anal. Appl. Pyrolysis* **2011**, *92*, 450−455.

(25) Marcilla, A.; Beltrán, M. I.; Navarro, R. *J. Anal. Appl. Pyrolysis* **2006**, *76*, 222−229.

(26) Guisnet, M.; Magnoux, P. *Appl. Catal.* **1989**, *54*, 1−27.

(27) Guisnet, M.; Costa, L.; Ramôa Ribeiro, F. *J. Mol. Catal. A: Chem.* **2009**, *305*, 69−83.

(28) Elordi, G.; Olazar, M.; Lopez, G.; Amutio, M.; Artetxe, M.; Aguado, R.; Bilbao, J. *J. Anal. Appl. Pyrolysis* **2007**, *79*, 450−455.

(29) Sie, S. *Ind. Eng. Chem. Res.* **1993**, *32*, 397−402.

(30) Park, J. W.; Kim, J. H.; Seo, G. *Polym. Degrad. Stab.* **2002**, *76*, 495.

(31) Schwidder, M.; Santhosh Kumar, M.; Bentrup, U.; Pérez-Ramírez, J.; Brückner, A.; Grünert, W. *Microporous Mesoporous Mater.* **2008**, *111*, 124−133.

(32) Zhang, J.; Chen, J.; Ren, J.; Sun, Y. *Appl. Catal., A* **2003**, *243*, 121−133.

(33) Busca, G. *Phys. Chem.* **1999**, *1*, 723−736.

(34) Pierella, L.; Saux, C.; Caglieri, S.; Bertorello, H.; Bercoff, P. *Appl. Catal., A* **2008**, *347*, 55−61.

(35) Bartholomew, C. H. *Appl. Catal., A* **2001**, *212*, 17−60.

(36) Marcilla, A.; Gómez-Siurana, A.; Valdes, F. *J. Anal. Appl. Pyrolysis* **2007**, *79*, 433−442.

(37) Micyus, N. J.; McCurry, J. D.; Seeley, J. V. *J. Chromatogr., A* **2005**, *1086*, 115−121.

(38) Abbot, J.; Guerzoni, F. N. *Appl. Catal.* **1992**, *85*, 173−188.